

## **SUPPLEMENTARY INFORMATION**

### **The use of radiocobalt as a label improves imaging of EGFR using DOTA-conjugated Affibody molecule**

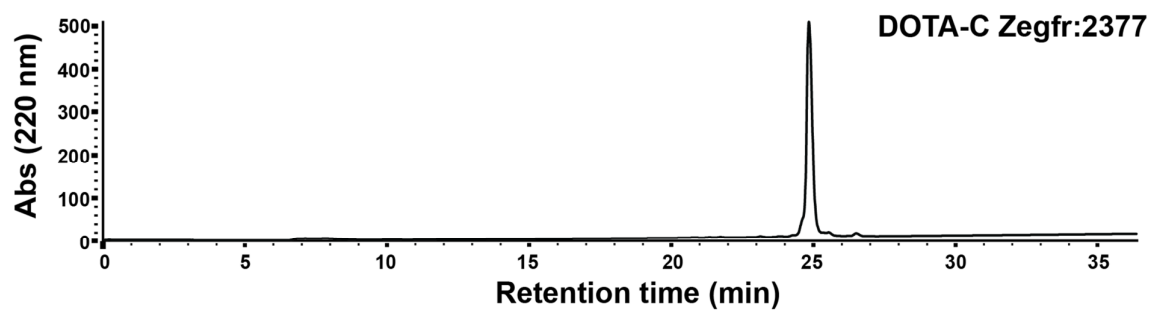
Javad Garousi<sup>1</sup>, Ken G. Andersson<sup>2</sup>, Johan H. Dam<sup>3</sup>, Birgitte B. Olsen<sup>3</sup>, Bogdan Mitran<sup>4</sup>, Anna Orlova<sup>4</sup>, Jos Buijs<sup>1</sup>, Stefan Ståhl<sup>2</sup>, John Löfblom<sup>2</sup>, Helge Thisgaard<sup>3</sup>, Vladimir Tolmachev<sup>1\*</sup>.

<sup>1</sup> Department of Immunology, Genetics and Pathology, Uppsala University, Uppsala, Sweden;

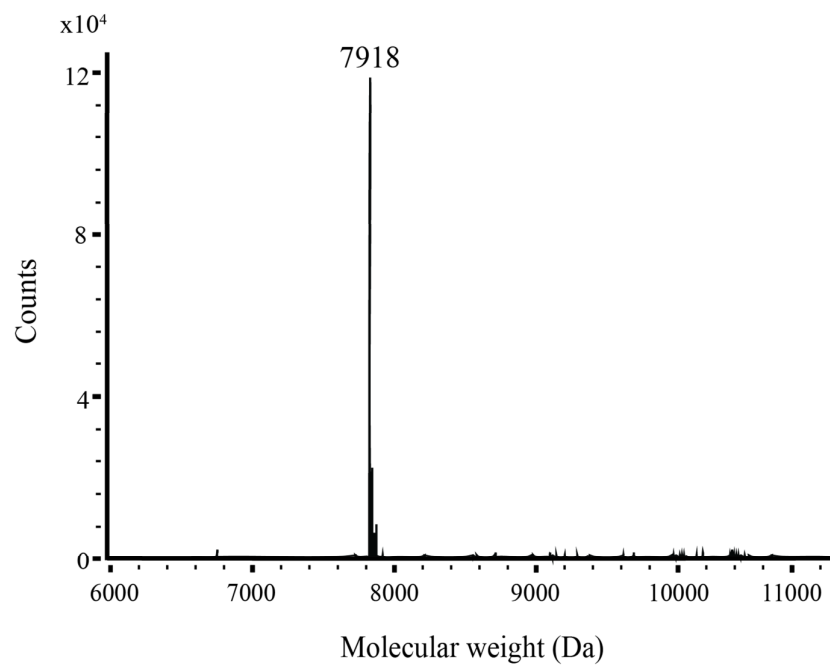
<sup>2</sup> Department of Protein Technology, KTH - Royal Institute of Technology, Stockholm, Sweden;

<sup>3</sup> Department of Nuclear Medicine, Odense University Hospital, Sdr. Boulevard 29, 5000 Odense, Denmark;

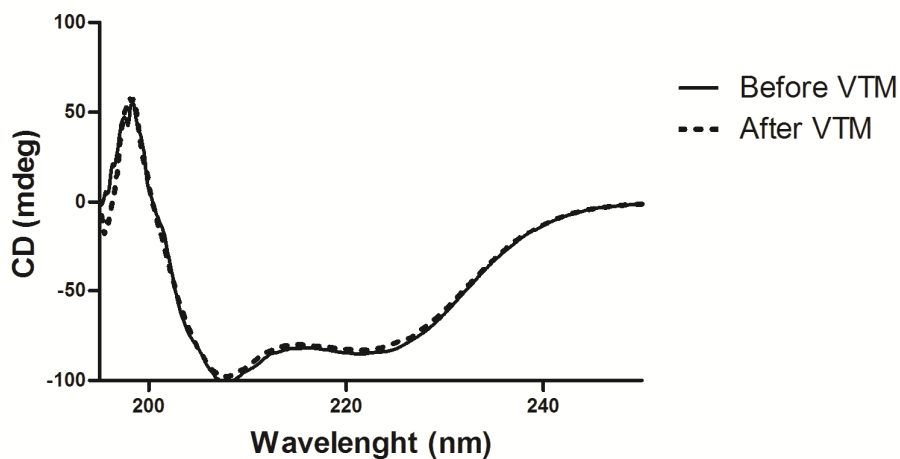
<sup>4</sup> Division of Molecular Imaging, Department of Medicinal Chemistry, Uppsala University, Uppsala, Sweden



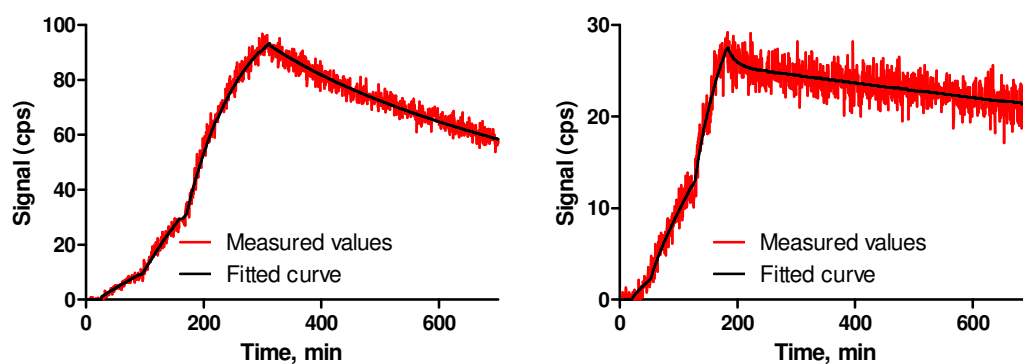
**Supplementary Figure S1.** Analytical RP-HPLC analysis of purified DOTA-Z<sub>EGFR:2377</sub>. The absorbance was measured at 220 nm.



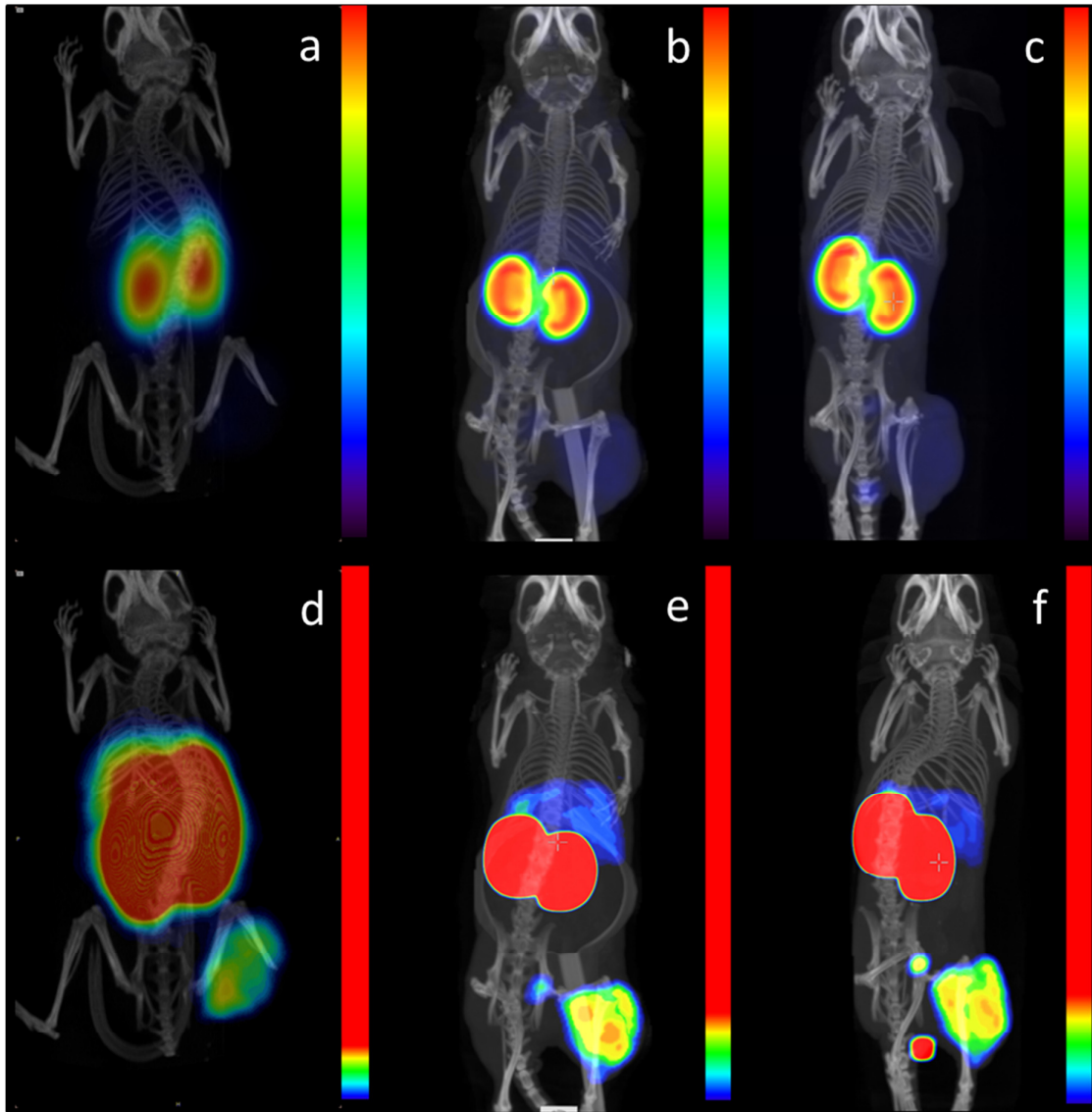
**Supplementary Figure S2.** Mass spectrum of purified DOTA-Z<sub>EGFR:2377</sub>.



**Supplementary Figure S3.** Overlay of circular dichroism spectra from 195- 250 nm for DOTA-Z<sub>EGFR:2377</sub> before (solid line) and after (dashed line) heating from 20-90°C.



**Supplementary Figure S4.** Representative sensorgrams of the LigandTracer measurement to determine the kinetics and affinity of <sup>111</sup>In- DOTA-Z<sub>EGFR:2377</sub> (left) and <sup>57</sup>Co-DOTA-Z<sub>EGFR:2377</sub> (right) to EGFR on A431 cells.



**Supplementary Figure S5.** PET/CT imaging using  $^{68}\text{Ga}$ -DOTA- $Z_{\text{EGFR}:2377}$  (a and d) and microSPECT/CT using  $^{57}\text{Co}$ -DOTA- $Z_{\text{EGFR}:2377}$  at 3 h (b and e) and 24 h (c and f) after injection of mice bearing EGFR-expressing A431 xenografts. The relative colour scales were normalized to the highest activity in images a, b and c, and then adjusted to provide first red pixel in tumours in images d, e and f (8, 13 and 17% of the full scale, respectively).

**Supplementary Table S1.** Radiochemical yields and specific activities of imaging probes used in this study.

	Yield, decay corrected; %	Max. specific activity at the end of synthesis; MBq/ $\mu$ g (GBq/ $\mu$ mol)
$^{57}\text{Co}$ -DOTA-Z <sub>EGFR:2377</sub>	> 99%	0.30 (2.34)
$^{55}\text{Co}$ -DOTA-Z <sub>EGFR:2377</sub>	> 99%	0.98 (7.05)
$^{68}\text{Ga}$ -DOTA-Z <sub>EGFR:2377</sub>	98.9 $\pm$ 0.5%	2.05 (16.3)

**Supplementary Table S2.** Long-lived positron-emitting radionuclides. Data are taken from

Tolmachev, V. & Stone-Elander S. Radiolabelled proteins for positron emission tomography: Pros and cons of labelling methods. *Biochim. Biophys. Acta.* **1800**, 487-510 (2010).

Nuclide	Half-life, hour	Mode of decay	Principal photon emissions, keV (abundance in %)
$^{55}\text{Co}$	17.5	$\beta^+$ 76 % EC 24 %	<b>511(152%)</b> , 477(20.2 %), 931(75 %), 1317(7.1%), 1408(16.9%)
$^{64}\text{Cu}$	12.7	$\beta^+$ 18 $\beta^-$ 37% EC 24 %	<b>511(36%)</b> , 1346(0.5%)
$^{76}\text{Br}$	16.2	$\beta^+$ 54% EC 46%	<b>511(108%)</b> , 559(74%), 657(15.9%), 1216(8.8%), 1854(14.7%), 2391(4.7%), 2792(5.6%), 2950.5(7.4%)
$^{86}\text{Y}$	14.7	$\beta^+$ 33 % EC 67 %	<b>511(66%)</b> , 443(16.9%), 628(32.6%), 646(9.2%), 703(15.4%), 778(22.4%), 1077(82.5%), 1153(30.5%), 1854(17.2%), 1920(20.8%)
$^{89}\text{Zr}$	78.4	$\beta^+$ 23% EC 77%	<b>511(46%)</b> , 909(100%)
$^{124}\text{I}$	100.2	$\beta^+$ 23% EC 77%	<b>511(46%)</b> , 603(61%), 723(9.96%), 1691(10.4%)